# NOTES AND CORRESPONDENCE

## Mapping of Airborne Doppler Radar Data

WEN-CHAU LEE

*National Center for Atmospheric Research,* Boulder, Colorado*

PETER DODGE AND FRANK D. MARKS JR.

*Hurricane Research Division, NOAA/AOML, Miami, Florida*

PETER H. HILDEBRAND

*National Center for Atmospheric Research,* Boulder, Colorado*

19 November 1992 and 9 August 1993

ABSTRACT

Two sets of equations are derived to 1) map airborne Doppler radar data from an aircraft-relative coordinate system to an earth-relative coordinate system, and 2) remove the platform motion from the observed Doppler velocities. These equations can be applied to data collected by the National Oceanic and Atmospheric Administration WP-3D system, the National Center for Atmospheric Research ELDORA system, and other airborne radar systems.

### 1. Introduction

The airborne Doppler radars on board the National Oceanic and Atmospheric Administration (NOAA) WP-3D airplanes have been used in studying the kinematic structures of Atlantic hurricanes (e.g., Marks and Houze 1984, 1987; Marks et al. 1992), convective storms (e.g., Hildebrand and Mueller 1985; Ray et al. 1985), squall lines and rainbands (e.g., Jorgensen et al. 1991; LeMone and Jorgensen 1991), and extratropical cyclones (e.g., Jorgensen et al. 1983; Wakimoto et al. 1992). Although the techniques for analyzing the airborne Doppler radar data are similar to those for the ground-based Doppler radar data, complexities arise due to the moving platform. Two additional steps must be performed on the airborne Doppler radar data before they can be interpreted or used in the dual-Doppler radar analysis. First, because the airborne Doppler radar measures the radial component of the target motion relative to the platform, the contribution from the platform motion has to be removed in order to obtain the radial component of the earth-relative target motion. Second, because the location of each data point is measured relative to the moving platform, the absolute location of each data point has to be known before the three-dimensional ground-relative winds can be synthesized. Both steps require knowledge of the aircraft location and beam pointing angle with sufficient accuracy, within 75 m and approximately 0.1° in order to retrieve the meteorological signal within the desired precision (Jorgensen et al. 1983; Testud and Hildebrand 1991).

Axford (1968) was the first to document a transformation matrix to compute the gust in a track-relative, horizontal platform using inertial navigation system (INS) data. Jorgensen et al. (1983) discussed the interpolation steps from a moving platform to a Cartesian coordinate system. Hildebrand et al. (1983) and Hildebrand and Mueller (1985) derived a simplified set of equations to remove the aircraft speed from the measured Doppler velocities and transform coordinates from a moving platform to a track-relative coordinate system. Heymsfield (1989) derived a transformation matrix to discuss the accuracy in the Doppler velocities observed by a vertical pointing airborne Doppler radar. Transformation equations applied directly to the NOAA WP-3D track-orthogonal scanning, airborne Doppler radar have been briefly documented in Jorgensen et al. (1983) and derived in several NOAA technical notes (e.g., DuGranrut 1988, personal communication; Marks 1989, personal communication). Different expressions of the transformation matrix exist because the terminologies and coordinate systems were defined differently in previous derivations. However, none of these papers presented a general transformation

* The National Center for Atmospheric Research is sponsored by the National Science Foundation.

*Corresponding author address:* Dr. Wen-Chau Lee, NCAR, P.O. Box 3000, Boulder, CO 80307-3000.

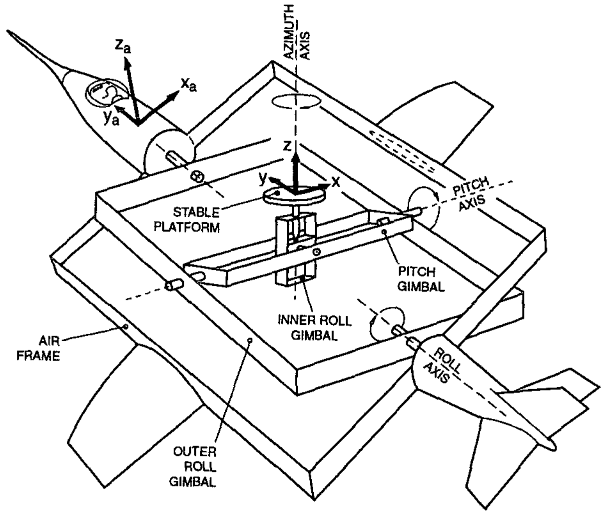


FIG. 1. Platform gimbals and reference frame [adapted from Axford (1968)].

matrix. With the installation and operation of the NOAA–CRPE (Centre de Recherche en Physique de l'Environnement) dual-beam antenna and the National Center for Atmospheric Research (NCAR)–CRPE ELDORA (Electra Doppler Radar)/ASTRAEA (analyse stereoscopique par radar aeroporte sur Electra) dual-Doppler radar system, there is an immediate need for a comprehensive derivation of the airborne Doppler radar coordinate transformation that has not been documented in the literature.

The goals of this paper are to 1) define the convention of angles involved in the coordinate systems, 2) derive the track-relative tilt angle for each beam in order to remove the aircraft ground speed from the measured Doppler velocities, 3) derive a transformation matrix between the moving aircraft platform and the earth-relative coordinate system to determine the absolute location of each pulse volume, and 4) derive the expression for Doppler velocity in terms of the aircraft attitudes, hydrometeor's motion, and motion of the platform from an airborne Doppler radar equipped with an INS.

## 2. Coordinate systems

The coordinate systems used here are all right-handed and orthogonal. In a right-handed coordinate system, angles are positive when they correspond to counterclockwise rotations about an axis perpendicular to the plane when looking along the axis toward the origin (Marion 1970). For example, in the Cartesian coordinate system commonly used in meteorology a positive angle in the $x$–$y$, $x$–$z$, and $y$–$z$ planes corresponds to rotation from east to north, from east to nadir, and from north to zenith, respectively. The coordinate systems we use are defined as follows (all parameters are listed in the Appendix):

1) Airframe relative ($\mathbf{X}_a$): $+x_a$ along right wing, $+y_a$ along the fuselage through nose, and $+z_a$ up along the tail stabilizer. The unit vectors are $\mathbf{i}_a$, $\mathbf{j}_a$, and $\mathbf{k}_a$.

2) Track relative, level ($\mathbf{X}_t$): $+y_t$ points along the track, the motion vector of the aircraft projected on the horizontal plane, $+x_t$ points 90° to the right of the $+y_t$ in the horizontal plane, and $+z_t$ points to the local zenith. The unit vectors are $\mathbf{i}_t$, $\mathbf{j}_t$, and $\mathbf{k}_t$.

3) Earth-relative, level ($\mathbf{X}$): $+y$ points to the north, $+x$ points to the east, and $+z$ to the local zenith. The unit vectors are $\mathbf{i}$, $\mathbf{j}$, and $\mathbf{k}$.

The airframe-relative coordinate system is defined by three INS attitude angles: pitch, roll, and heading; a fourth parameter, track, is calculated by integrating three accelerometers with time. These attitude angles are defined in the meteorological convention. A schematic of the INS rotation gimbals is presented in Fig.

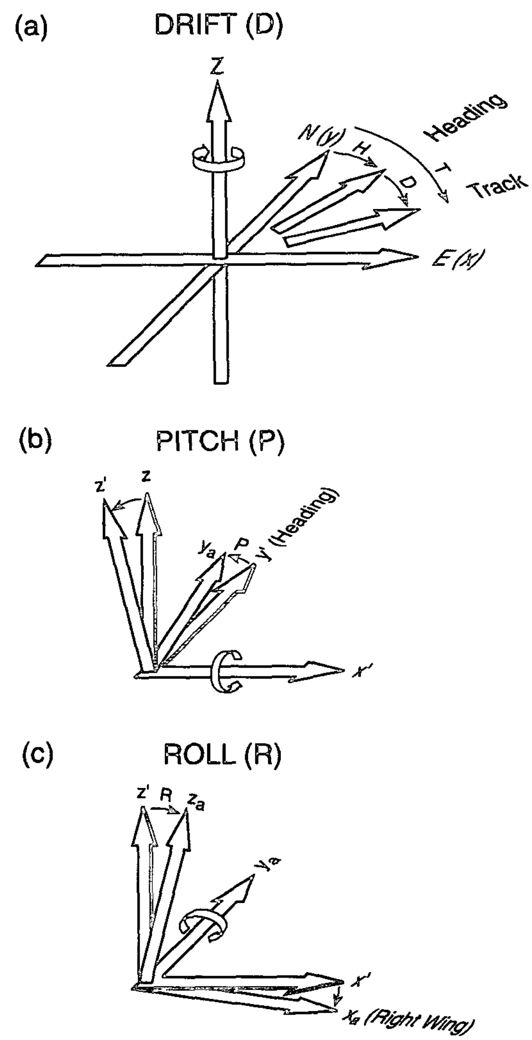


FIG. 2. Definitions of the INS attitude angles, (a) heading ($H$), track ($T$), and drift ($D$) angles; (b) pitch ($P$) angle; and (c) roll ($R$) angle.

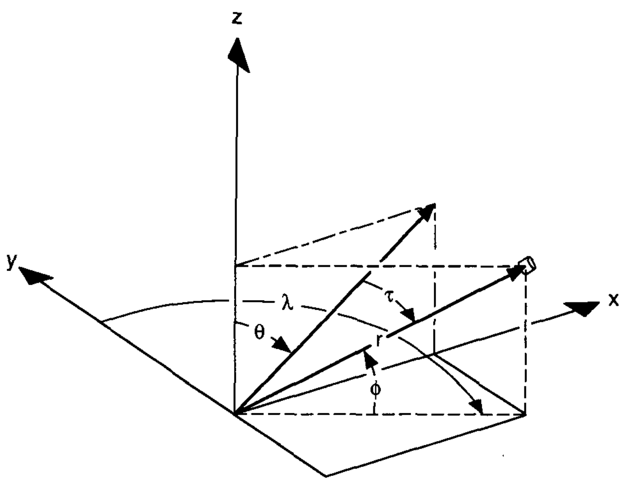


FIG. 3. Definitions of the azimuth λ, elevation $\phi$, rotation angle $\theta$, and tilt angle $\tau$ in the earth-relative coordinate system. The subscript $t$ can be added to represent quantities in the track-relative coordinate system or replaced by $a$ to represent quantities in the aircraft-relative coordinate system.

1 [adapted from Axford (1968)]. The order of rotation from a track-relative coordinate system to an aircraft-relative coordinate system is drift, pitch, and roll, due to the design of the INS. The heading $H$ of an aircraft is the angle measured clockwise from north to the projection of the aircraft's longitudinal axis on the horizontal plane. The track $T$ is the angle measured clockwise from the north to the aircraft ground trajectory, also on the horizontal plane (Fig. 2a). The drift angle $D$ is the angle between the heading and the track angles. A positive drift angle is defined as the track more clockwise than the heading; hence, $D = T - H$. As a result, rotations on positive $H$, $T$, and $D$ represent negative rotations in the above mathematical coordinate systems. Pitch $P$ is the angle that the aircraft longitudinal axis makes with the horizontal plane. Pitch is denoted as positive when the nose is up. This is the same convention used in the Cartesian system (Fig. 2b). Roll $R$ is the angle that the wings make with the horizontal plane where the positive angle is the rotation about the aircraft longitudinal axis when the right wing is down (Fig. 2c).

The three attitude angles (or INS gimbals) are *not* all measured as rotations about axes of the $\mathbf{X}_a$ coordinate system. Roll is measured about $y_a$, but pitch is a rotation about $x'$, and heading (or drift) is a rotation about $z$, where $x'$, $y'$, and $z'$ are in intermediate coordinate systems. Because of these characteristics of the INS, intermediate angles need not be calculated; taken in the order roll, pitch, and drift, the attitude angles are the Eulerian angles (Marion 1970) of the transformation from $X_a$ to $X_t$.

The location of each radar data point is measured in the aircraft-relative coordinate system in terms of a rotation angle $\theta_a$, a tilt angle $\tau_a$, and a range $r$. The rotation angle is defined as the projection of the radar beam onto a plane perpendicular to the fuselage (i.e., $x_a$–$z_a$ plane) as illustrated in Fig. 3. The rotation angle $\theta_a$ increases clockwise from $+y_a$, where 0 is the $+z_a$ axis and $\pi/2$ is the $+x_a$ axis. The tilt angle $\tau_a$ is defined as the deviation of the radar beam from the $x_a$–$z_a$ plane. The tilt angle $\tau_a$ is positive (negative) when the radar tilts fore (aft). The azimuth λ is defined as the clockwise angle between the north and the horizontal projection of the radar beam. The elevation $\phi$ is the angle on a vertical plane between the radar beam and the horizontal plane.

## 3. Coordinate transformation

The transformation matrices for rotations of positive angle $\zeta$, $\eta$, and $\xi$ about the $z$, $y$, and $x$ axes, respectively, in a right-handed Cartesian coordinate system are given by Foley et al. (1990, 214–215) and Marion (1970, 13–18):

$$\mathbf{M}_z = \begin{pmatrix} \cos\zeta & \sin\zeta & 0 \\ -\sin\zeta & \cos\zeta & 0 \\ 0 & 0 & 1 \end{pmatrix}, \tag{1}$$

$$\mathbf{M}_y = \begin{pmatrix} \cos\eta & 0 & -\sin\eta \\ 0 & 1 & 0 \\ \sin\eta & 0 & \cos\eta \end{pmatrix}, \tag{2}$$

$$\mathbf{M}_x = \begin{pmatrix} 1 & 0 & 0 \\ 0 & \cos\xi & \sin\xi \\ 0 & -\sin\xi & \cos\xi \end{pmatrix}. \tag{3}$$

The corresponding aircraft-relative Cartesian components, $x_a$, $y_a$, $z_a$, of a vector, $r$, $\theta_a$, $\tau_a$, are

$$\begin{pmatrix} x_a \\ y_a \\ z_a \end{pmatrix} = r \begin{pmatrix} \cos\tau_a \sin\theta_a \\ \sin\tau_a \\ \cos\theta_a \cos\tau_a \end{pmatrix}. \tag{4}$$

The transformation from the aircraft-relative coordinate system $\mathbf{X}_a$ to the track-relative coordinate system $\mathbf{X}_t$ involves three successive rotations in the order of roll, pitch, and drift. The first rotation is about the $y_a$ axis by rotating the $x_a$ axis clockwise to the $x'$ axis (Fig. 2c), which is equivalent to rotating $-R$ in a right-handed coordinate system. The conversion matrix $\mathbf{M}_R$ is made by replacing $\eta$ with $-R$ in (2):

$$\mathbf{M}_R = \begin{pmatrix} \cos R & 0 & \sin R \\ 0 & 1 & 0 \\ -\sin R & 0 & \cos R \end{pmatrix}. \tag{5}$$

The resulting axes of this rotation are $x'$, $y_a$, and $z'$.

The second rotation (pitch $P$) is about the $x'$ axis (Fig. 2b) by rotating the $y_a$ axis clockwise to the $y'$ axis which is equivalent to rotating $-P$ in a right-handed coordinate system. Substituting $\xi$ with $-P$ in (3), the conversion matrix $\mathbf{M}_P$ is

$$\mathbf{M}_P = \begin{pmatrix} 1 & 0 & 0 \\ 0 & \cos P & -\sin P \\ 0 & \sin P & \cos P \end{pmatrix}. \quad (6)$$

The resulting axes of this rotation are $x'$, $y'$, $z_t$. Here, $y'$ is along the heading of the aircraft, and $x'$ is 90° to the right of the $y'$ axis. This intermediate coordinate system is a leveled, heading-relative coordinate system. Note that $z_t$ coincides with $z$. The subscript $t$ in $z_t$ will be omitted in the following equations.

The final rotation about the $z$ axis completes the transformation into the leveled track-relative system $\mathbf{X}_t$ (Fig. 2a). Because a positive drift $D$ denotes track to the right of the heading, a clockwise rotation of $D$ on the $x$–$y$ plane is equivalent to a $-D$ rotation. Substituting $-D$ in (1), the conversion matrix $\mathbf{M}_D$ is

$$\mathbf{M}_D = \begin{pmatrix} \cos D & -\sin D & 0 \\ \sin D & \cos D & 0 \\ 0 & 0 & 1 \end{pmatrix}. \quad (7)$$

The transformation between $\mathbf{X}_a$ and $\mathbf{X}_t$ in the matrix form becomes

$$\mathbb{X}_t = \mathbb{M}_D \mathbb{M}_P \mathbb{M}_R \mathbb{X}_a. \quad (8)$$

Regroup and expand (8), and apply (4) to get

$$\begin{pmatrix} x_t \\ y_t \\ z \end{pmatrix} = [\mathbb{M}_D \mathbb{M}_P]\left[\mathbb{M}_R \begin{pmatrix} x_a \\ y_a \\ z_a \end{pmatrix}\right]$$

$$= r\begin{pmatrix} \cos D & -\sin D \cos P & \sin D \sin P \\ \sin D & \cos D \cos P & -\cos D \sin P \\ 0 & \sin P & \cos P \end{pmatrix} \times \begin{pmatrix} \cos\tau_a \sin(\theta_a + R) \\ \sin\tau_a \\ \cos\tau_a \cos(\theta_a + R) \end{pmatrix}.$$

Therefore, the transformation equations in the matrix form are

$$\begin{pmatrix} x_t \\ y_t \\ z \end{pmatrix} = r\begin{pmatrix} \cos(\theta_a + R)\sin D \cos\tau_a \sin P + \cos D \sin(\theta_a + R)\cos\tau_a - \sin D \cos P \sin\tau_a \\ -\cos(\theta_a + R)\cos D \cos\tau_a \sin P + \sin D \sin(\theta_a + R)\cos\tau_a + \cos P \cos D \sin\tau_a \\ \cos P \cos\tau_a \cos(\theta_a + R) + \sin P \sin\tau_a \end{pmatrix}. \quad (9)$$

The track-relative rotation, tilt, azimuth, and elevation angles are thus

$$\theta_t = \tan^{-1}\frac{x_t}{z}, \quad (10)$$

$$\tau_t = \sin^{-1}\frac{y_t}{r}, \quad (11)$$

$$\lambda_t = \tan^{-1}\frac{x_t}{y_t}, \quad (12)$$

$$\phi_t = \sin^{-1}\frac{z}{r}. \quad (13)$$

These angles are of particular interest for the NOAA WP-3D tail antenna because it can scan perpendicular to the flight track. The tilt angle of the radar must be adjusted dynamically in order for the radar to scan orthogonal to the track, up to drift angles of ±25°, because of the limitations in the P-3 antenna. The radar tilt angle $\tau_a$ can be predicted from a given drift, pitch, and roll angle of the aircraft. The coordinate transformation from $\mathbf{X}_t$ to $\mathbb{X}_a$ is exactly the inverse of the transformation derived above. Because the matrix is orthogonal, the inverse is simply the transpose of the original matrix.

For the French dual-beam antenna, the ELDORA antenna, and the WP-3D antenna operated in the Fore/Aft Scanning Mode (Jorgensen and DuGranrut 1991), the track-relative tilt angle $\tau_t$ is important. The component of the aircraft ground speed $V_g$ in the beam direction is $-V_g \sin\tau_t$. Knowledge of $\tau_t$ is required to properly remove the ground velocity component in the Doppler velocity.

Finally, it is necessary to obtain the earth-relative azimuth $\lambda$ and elevation angle $\phi$. This requires an additional matrix, $\mathbb{M}_T$, which counterclockwise rotates a coordinate system along the $z$ axis by $T$. Replacing $\zeta$ with $T$ in (1) gives

$$\mathbb{M}_T = \begin{pmatrix} \cos T & \sin T & 0 \\ -\sin T & \cos T & 0 \\ 0 & 0 & 1 \end{pmatrix}.$$

The resulting matrix representation is

$$\mathbb{X} = \mathbb{M}_T \mathbb{M}_D \mathbb{M}_P \mathbb{M}_R \mathbb{X}_a.$$

Note that

$$\mathbf{M}_T \mathbf{M}_D = \begin{pmatrix} \cos T & \sin T & 0 \\ -\sin T & \cos T & 0 \\ 0 & 0 & 1 \end{pmatrix}\begin{pmatrix} \cos D & -\sin D & 0 \\ \sin D & \cos D & 0 \\ 0 & 0 & 1 \end{pmatrix}$$

$$= \begin{pmatrix} \cos T\cos D + \sin T\sin D & -\cos T\sin D + \sin T\cos D & 0 \\ -\sin T\cos D + \sin D\cos T & \sin T\sin D + \cos T\cos D & 0 \\ 0 & 0 & 1 \end{pmatrix}$$

$$= \begin{pmatrix} \cos(D-T) & -\sin(D-T) & 0 \\ \sin(D-T) & \cos(D-T) & 0 \\ 0 & 0 & 1 \end{pmatrix}. \quad (14)$$

Comparing (7) and (14), one can obtain $x$, $y$, and $z$ by replacing $D$ with $D - T$ and substituting $D - T$ with $-H$ in (9) gives

$$\begin{pmatrix} x \\ y \\ z \end{pmatrix} = r\begin{pmatrix} -\cos(\theta_a + R)\sin H\cos\tau_a\sin P + \cos H\sin(\theta_a + R)\cos\tau_a + \sin H\cos P\sin\tau_a \\ -\cos(\theta_a + R)\cos H\cos\tau_a\sin P - \sin H\sin(\theta_a + R)\cos\tau_a + \cos P\cos H\sin\tau_a \\ \cos P\cos\tau_a\cos(\theta_a + R) + \sin P\sin\tau_a \end{pmatrix}. \quad (15)$$

In effect, instead of rotating $-D$ in (7) to get to a track-relative coordinate system, (15) can be obtained by counterclockwise rotation of $H$ directly to the earth-relative coordinate system.

The earth-relative azimuth and elevation angle are

$$\lambda = \tan^{-1}\frac{x}{y}, \quad (16)$$

$$\phi = \sin^{-1}\frac{z}{r}. \quad (17)$$

For computational efficiency, it is easier to obtain $\lambda$ and $\phi$ directly from $\lambda_t$ and $\phi_t$:

$$\lambda = \lambda_t + T,$$

$$\phi = \phi_t.$$

## 4. Expression of the Doppler velocity

The velocity measured by the airborne Doppler radar includes components of motion from both the hydrometeor and the platform. The motion vector of the hydrometeors can be written as

$$\mathbf{V} = \mathbf{i}u + \mathbf{j}v + \mathbf{k}(w - v_t), \quad (18)$$

where $u$, $v$, and $w$ are the three Cartesian components of air motion in the earth-relative coordinate system and $v_t$ is the terminal fall speed of the hydrometeors, positive downward. The motion vector of the aircraft is

$$\mathbf{V}_g = \mathbf{i}\mathrm{VG}\sin T + \mathbf{j}\mathrm{VG}\cos T + \mathbf{k}\mathrm{WG}, \quad (19)$$

where VG and WG are the horizontal and vertical ground speeds of the aircraft, respectively.

If the pitch and heading are changing with time and the INS is located some distance $L$ away from the antenna, there is an additional apparent antenna motion $\mathbf{V}_a$ due to the momentum arm ($Ld\mathbf{P}/dt \neq 0$ and/or $Ld\mathbf{H}/dt \neq 0$). Here, $\mathbf{H}$ and $\mathbf{P}$ are the unit vectors for heading and pitch, which can be expressed as follows:

$$\mathbf{H} = \mathbf{i}\sin H + \mathbf{j}\cos H, \quad (20)$$

$$\mathbf{P} = \mathbf{i}\cos P\sin H + \mathbf{j}\cos P\cos H + \mathbf{k}\sin P, \quad (21)$$

and their derivatives are as follows:

$$\frac{d\mathbf{H}}{dt} = \mathbf{i}\cos H\frac{dH}{dt} - \mathbf{j}\sin H\frac{dH}{dt}, \quad (22)$$

$$\frac{d\mathbf{P}}{dt} = \mathbf{i}\left(-\sin P\sin H\frac{dP}{dt} + \cos P\cos H\frac{dH}{dt}\right) + \mathbf{j}\left(-\sin P\cos H\frac{dP}{dt} - \cos P\sin H\frac{dH}{dt}\right) + \mathbf{k}\cos P\frac{dP}{dt}. \quad (23)$$

The apparent antenna motion $\mathbf{V}_a$ is

$$\mathbf{V}_a = -\left(L\frac{d\mathbf{H}}{dt} + L\frac{d\mathbf{P}}{dt}\right)$$

$$= -\left[L(1 + \cos P)\frac{dH}{dt}(\mathbf{i}\cos H - \mathbf{j}\sin H) + \frac{dP}{dt}(-\mathbf{i}\sin P\sin H - \mathbf{j}\sin P\cos H + \mathbf{k}\cos P)\right]$$

$$= -L\left\{\mathbf{i}\left[\cos H(1+\cos P)\frac{dH}{dt} - \sin P \sin H \frac{dP}{dt}\right] - \mathbf{j}\left[\sin H(1+\cos P)\frac{dH}{dt} + \sin P \cos H \frac{dP}{dt}\right] + \mathbf{k}\cos P \frac{dP}{dt}\right\}. \quad (24)$$

The negative sign in (24) reflects the fact that the antenna moves in the opposite direction as $d\mathrm{H}/dt$ and $d\mathrm{P}/dt$. For $L = 29.8$ m in the NCAR ELDORA system, $1°\ \mathrm{s}^{-1}$ change in heading and/or pitch produces a 0.5 m $\mathrm{s}^{-1}$ apparent antenna motion. During a smooth straight-line flight pattern without much crosswind shear, this apparent antenna motion is small and can be ignored; however, the apparent antenna motion is significant when the aircraft is changing altitude and/or heading. During a turn in one of the TOGA COARE (Tropical Ocean Global Atmosphere Coupled Ocean–Atmosphere Response Experiment) flights, typical values for $dH/dt$ and $dP/dt$ were 1.5 and $1°\ \mathrm{s}^{-1}$, respectively. The extreme value for $dP/dt$ can be $4°\ \mathrm{s}^{-1}$, where the effect of the apparent motion cannot be ignored.

The measured Doppler velocity $V_r$ can then be expressed as

$$V_r = \mathbb{V}\cdot\mathbb{e}_r - \mathbb{V}_g\cdot\mathbb{e}_r - \mathbb{V}_a\cdot\mathbb{e}_r, \quad (25)$$

where $\mathbf{e}_r = (x\mathbb{i} + y\mathbb{j} + z\mathbb{k})/r$ is the unit vector pointing along the radar beam. The ground speed component is subtracted because aircraft motion causes an apparent motion of the hydrometeors in the opposite direction. Expanding and simplifying (25) with (17),

$$V_r = \frac{1}{r}(ux+vy) + (w - v_t - \mathrm{WG})\sin\phi - \frac{\mathrm{VG}}{r}(x\sin T + y\cos T) + \frac{L}{r}\left\{x\left[(1+\cos P)\cos H\frac{dH}{dt} - \sin P\sin H\frac{dP}{dt}\right] - y\left[(1+\cos P)\sin H\frac{dH}{dt} + \sin P\cos H\frac{dP}{dt}\right] + z\cos P\frac{dP}{dt}\right\}. \quad (26)$$

From (11), $y_t/r = \sin\tau_t$, and from the coordinate transformation between $\mathbb{X}_t$ and $\mathbb{X}$, $y_t = x\sin T + y\cos T$, we obtain $(x/r)\sin T + (y/r)\cos T = \sin\tau_t$. So, (26) reduces to

$$V_r = \frac{1}{r}(ux+vy) + (w - v_t - \mathrm{WG})\sin\phi - \mathrm{VG}\sin\tau_t + \frac{L}{r}\left\{(1+\cos P)(x\cos H - y\sin H)\frac{dH}{dt} - [\sin P(x\sin H + y\cos H) - z\cos P]\frac{dP}{dt}\right\}. \quad (27)$$

Using (15), the hydrometeor's Doppler velocity, $\mathbb{V}\cdot\mathbb{e}_r$ can be expressed in terms of tilt, elevation, heading, drift, pitch, roll, rotation angle, platform motion ($\mathbb{V}_g\cdot\mathbb{e}_r$ and $\mathbb{V}_a\cdot\mathbf{e}_r$), and the Doppler velocity $V_r$. Given independent measurements of $V_r$ of the same pulse volume from different angles, one can estimate $u$, $v$, and $w$ as described in Marks and Houze (1984) and Ray et al. (1985).

## 5. Summary

This paper derives expressions for the radial velocity, measured by an airborne Doppler radar, and the equations for coordinate transformation among the aircraft-relative coordinates $\mathbb{X}_a$, the track-relative coordinates $\mathbb{X}_t$, and the earth-relative coordinate $\mathbb{X}$. These equations will allow for the removal of the ground speed from the observed Doppler velocity and the calculation of the corresponding azimuth and elevation angles for future use in the multiple-Doppler radar analysis. With the correct radar coordinates (rotation angle, tilt angle, range), INS information (drift, pitch, roll, and heading), aircraft altitude and ground speed, the Doppler velocity of the ground gates [the gate(s) that intersect the ground on each beam] should be zero. However, experience has shown that they are not necessarily zero due to the uncertainties embedded within the INS data and mounting errors of the radar that will introduce errors in the Doppler velocities. A method to identify these biases has been documented in Testud and Hildebrand (1991).

*Acknowledgments.* J. Hackney helped code software. M. Carpenter made helpful suggestions. Comments from J. Testud and two anonymous reviewers led to improvement and clarity of this manuscript.

## APPENDIX

### Parameter List

$\mathbf{X}_a$: Airframe-relative coordinate system $(x_a, y_a, z_a)$
$\mathbf{X}_t$: Level track-relative coordinate system $(x_t, y_t, z_t)$
$\mathbf{X}$: Level earth-relative coordinate system $(x, y, z)$
$H$: Heading of the aircraft
$T$: Track of the aircraft
$D$: Drift angle
$P$: Pitch angle
$R$: Roll angle
$\lambda$: Azimuth angle
$\phi$: Elevation angle
$\theta$: Rotation angle
$\tau$: Tilt angle
$L$: Distance between INS and the antenna
$\mathbf{V}$: Motion vector of the hydrometeor $(u, v, w)$
$v_t$: Terminal fall speed of the hydrometeor, positive downward
$\mathbf{V}_g$: Aircraft ground speed, has magnitude VG and direction $T$
$\mathbf{V}_a$: Apparent antenna motion vector
$V_r$: Doppler velocity
$\mathbf{e}_r$: Unit vector pointing along the radar beam

## REFERENCES


Axford, D. N., 1968: On the accuracy of wind measurements using an inertial platform in an aircraft, and an example of a measurement of the vertical mesostructure of the atmosphere. *J. Appl. Meteor.*, **7**, 645–666.

Foley, J. D., A. Van Dam, S. K. Feiner, and J. F. Hughes, 1990: *Computer Graphics, Principles and Practice.* Addison-Wesley, 1174 pp.

Heymsfield, G. M., 1989: Accuracy of vertical air motions from nadir-viewing Doppler airborne radars. *J. Atmos. Oceanic Technol.*, **6**, 1079–1082.

Hildebrand, P. H., and C. K. Mueller, 1985: Evaluation of meteorological airborne radar. Part I: Dual-Doppler analyses of air motions. *J. Atmos. Oceanic Technol.*, **2**, 362–380.

——, C. Walther, C. L. Frush, and C. K. Mueller, 1983: Airborne Doppler weather radar: Evaluation and discussion of applications. Preprints, *21st Conf. on Radar Meteorology,* Edmonton, Canada, Amer. Meteor. Soc., 270–277.

Jorgensen, D. P., and J. D. DuGranrut, 1991: A dual-beam technique for deriving wind fields from airborne Doppler radar. Preprints, *25th Int. Conf. on Radar Meteorology,* Paris, Amer. Meteor. Soc., 458–461.

——, P. H. Hildebrand, and C. L. Frush, 1983: Feasibility test of an airborne pulse-Doppler meteorological radar. *J. Climate Appl. Meteor.*, **22**, 744–757.

——, M. A. LeMone, and B. J.-D. Jou, 1991: Precipitation and kinematic structure of an oceanic mesoscale convective system. Part I: Convective line structure. *Mon. Wea. Rev.*, **119**, 2608–2637.

LeMone, M. A., and D. P. Jorgensen, 1991: Precipitation and kinematic structure of an oceanic mesoscale convective system. Part II: Momentum transport and generation. *Mon. Wea. Rev.*, **119**, 2638–2653.

Marion, J. B., 1970: *Classical Dynamics of Particles and Systems.* Academic Press, 573 pp.

Marks, F. D., and R. A. Houze, 1984: Airborne Doppler radar observations in Hurricane Debby. *Bull. Amer. Meteor. Soc.*, **65**, 569–582.

——, and ——, 1987: Inner core structure of Hurricane Alicia from Doppler radar observations. *J. Atmos. Sci.*, **44**, 1296–1317.

——, ——, and J. F. Gamache, 1992: Dual-aircraft investigation of the inner core of Hurricane Norbert. Part I: Kinematic structure. *J. Atmos. Sci.*, **49**, 919–942.

Ray, P. S., D. P. Jorgensen, and S.-L. Wang, 1985: Airborne Doppler radar observations of a convective storm. *J. Climate Appl. Meteor.*, **24**, 688–698.

Testud, J., and P. H. Hildebrand, 1991: A technique to correct airborne Doppler data for coordinate transformation errors using surface clutter. Preprints, *25th Int. Conf. on Radar Meteorology,* Paris, Amer. Meteor. Soc., 493–496.

Wakimoto, R. M., W. Blier, and C. Liu, 1992: The frontal structure of an explosive ocean cyclone: Airborne radar observations of ERICA IOP 4. *Mon. Wea. Rev.*, **120**, 1135–1155.